

Direct Evidence for Dynamic Electron-Electron Coulomb Correlations in Metals

F. Green, D. N. Lowy, and J. Szymański

School of Physics, The University of New South Wales, Kensington, Sydney 2033, Australia

(Received 21 September 1981)

A microscopic calculation for the electron gas which is parameter free and satisfies the sum rules predicts twin peaks in the dynamic structure factor which are in substantial quantitative agreement with reported measurements on Be and Al. The twin peaks are generated by dynamic Coulomb correlations between pairs of electrons. No evidence is seen of a corresponding maximum in the pair correlation function.

PACS numbers: 71.45.Gm, 78.70.Ck

Some years ago Platzman and Eisenberger¹ reported experimental measurements of the dynamic structure factor $S(\vec{q}, \omega)$ for inelastic x-ray scattering at high momentum transfers off certain metals. At momentum transfers \vec{q} which were somewhat larger than the Fermi momentum k_F of the conduction electrons, $S(\vec{q}, \omega)$ exhibited a puzzling two-peak structure as a function of ω . This same structure is observed for a number of different metals (Al, Be, Li, and Mg) with comparable conduction-electron densities, and so one must conclude that the effect is due to properties of the interacting conduction-electron gas rather than some peculiar band-structure effect.

There have been several attempts to explain this structure²⁻⁵ none of which has been very satisfactory. Only upon the introduction of the single-particle lifetime was the double peak obtained^{2,3} (see also Ref. 4). However, the very possibility of producing such a structure with use of on-shell electron self-energies has been questioned⁶; nor is it clear how the sum rules can be preserved⁴ when lifetimes are introduced in an *ad hoc* manner.² In the only apparently consistent model employing the memory function formalism³ the authors were forced to introduce freely adjustable parameters. Finally, the identification of the second peak as the remnant of the collective plasmon excitation² is speculative, and questionable on the grounds that the wave-

length q^{-1} is shorter than the interparticle spacing.

In this Letter we stress that the complicated two-peak structure arises from strong correlations between interacting pairs of electrons, and that it does not derive from collective effects. We report some quantitative agreement between the experimental measurements and the predictions of a calculation which uses a straightforward extension of the theory for electron-electron correlations proposed by Lowy and Brown.⁷ The theory constructs a two-body effective interaction for electrons in an electron gas which takes into account in a pairwise fashion the non-local dynamic Coulomb scattering occurring between electrons at small separations. This short-range interaction is then incorporated into a screening theory by appropriately modifying the irreducible density-density response function $\chi_{sc}(\vec{q}, \omega)$ ⁸ so that it includes correlated two-particle scattering.

We start by defining the nonlocal, dynamic interaction $\langle \vec{q}, \vec{K} | t_{ee} | \vec{k}, \vec{K} \rangle$ for two electrons undergoing multiple scattering with a bare Coulomb interaction v in the presence of a quiescent Fermi sea. This is given by the solution of the Bethe-Goldstone integral equation.⁷ The state $|\vec{q}, \vec{K}\rangle$ is a two-particle plane wave with relative momentum \vec{q} and center-of-mass momentum \vec{K} .

We include the effect of two-particle scattering in the irreducible part of the density-density response function $\chi_{sc}(\vec{q}, \omega)$ (see Fig. 1):

$$\chi_{sc}(\vec{q}, \omega) = \chi_0(\vec{q}, \omega) + \chi_2(\vec{q}, \omega), \quad (1)$$

$$\begin{aligned} \chi_2(\vec{q}, \omega) = & \int \frac{d^4 k_1}{(2\pi)^4} \int \frac{d^4 k_2}{(2\pi)^4} G_0(k_1) G_0(k_1 + q) G_0(k_2) G_0(k_2 - q) [2 \langle \vec{q} + \vec{k}, \vec{K} | \bar{t}_{ee}(E_1) | \vec{k}, \vec{K} \rangle \\ & + \langle \frac{1}{2} \vec{K} + \frac{1}{2} \vec{q}, 2\vec{k} + \vec{q} | \bar{t}_{ee}(E_2) | \frac{1}{2} \vec{K} - \frac{1}{2} \vec{q}, 2\vec{k} + \vec{q} \rangle + \langle \frac{1}{2} \vec{K} + \frac{1}{2} q, 2\vec{k} + \vec{q} | \bar{t}_{ee}(E_3) | \frac{1}{2} \vec{K} - \frac{1}{2} \vec{q}, 2\vec{k} + \vec{q} \rangle], \end{aligned} \quad (2)$$

where $\chi_0(\vec{q}, \omega)$ is the density-density response function for the noninteracting system and $G_0(k)$ is the free-particle Green's function for the four-momentum k . The integrals over \vec{k}_1 and \vec{k}_2 are over the Fermi sea; $\vec{K} = \vec{k}_1 + \vec{k}_2$ and $\vec{k} = \frac{1}{2}(\vec{k}_1 - \vec{k}_2)$. The scattering amplitude is related to $\bar{t}_{ee}(E)$ by $\bar{t}_{ee}(E) = [t_{ee}(E) - v]$. After the integrations over k_1^0 and k_2^0 have been performed, the initial energies are given by E_1

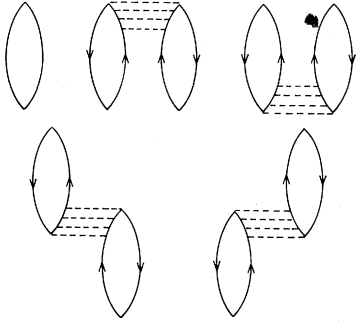


FIG. 1. Goldstone-diagram contributions to χ_{sc} . The first term is χ_0 . The ladders of bare Coulomb interactions are summed from two lines to infinity.

$= \epsilon_{k_1} + \epsilon_{k_2}$, $E_2 = E_1 + \omega$, and $E_3 = E_1 - \omega$, where ϵ_{k_1} is the single-particle energy for momentum k_1 .

$\chi_2(\vec{q}, \omega)$ is the irreducible contribution to $\chi_{sc}(\vec{q}, \omega)$ arising from two-particle scattering. The total density-density response function is given in terms of the irreducible response function by the exact relation⁸

$$\chi(\vec{q}, \omega) = \chi_{sc}(\vec{q}, \omega) / [1 - v(\vec{q})\chi_{sc}(\vec{q}, \omega)]. \quad (3)$$

In the random-phase approximation (RPA) $\chi_{sc}(\vec{q}, \omega)$ is approximated simply by $\chi_0(\vec{q}, \omega)$. However, as we shall see, it is crucial to the final form of our results that the imaginary part of $\chi_{sc}(\vec{q}, \omega)$ has a different structure from $\text{Im}\chi_0(\vec{q}, \omega)$. This is of course due to the fact that our $\chi_{sc}(\vec{q}, \omega)$ includes the effect of correlated two-particle scattering. This allows for real two-electron excitations which can permanently carry off energy-momentum (\vec{q}, ω) from the incoming x ray.

The dynamic structure factor $S(\vec{q}, \omega)$ is related to $\chi(\vec{q}, \omega)$ through the expression $S(\vec{q}, \omega) = -[\text{Im}\chi(\vec{q}, \omega)]/\pi$. In Fig. 2 we show our calculated $S(\vec{q}, \omega)$. Also shown is the calculated $S(\vec{q}, \omega)$ using RPA, and $S(\vec{q}, \omega)$ as measured in Ref. 1.

The distinctive two-peak structure that we see in our results stems directly from the behavior of the irreducible two-particle scattering term $\chi_2(\vec{q}, \omega)$. As a function of ω for fixed \vec{q} , $\text{Im}\chi_2(\vec{q}, \omega)$ exhibits a marked dip near the point where $\text{Im}\chi_0(\vec{q}, \omega)$ is a maximum. The amplitude of the corresponding two-particle wave function when averaged over all the electrons in the Fermi sea becomes very small, indicating that the two-particle correlations due to the Coulomb potential are particularly efficient here. We come to the remarkable conclusion that the twin-peak structure can be directly associated with corre-

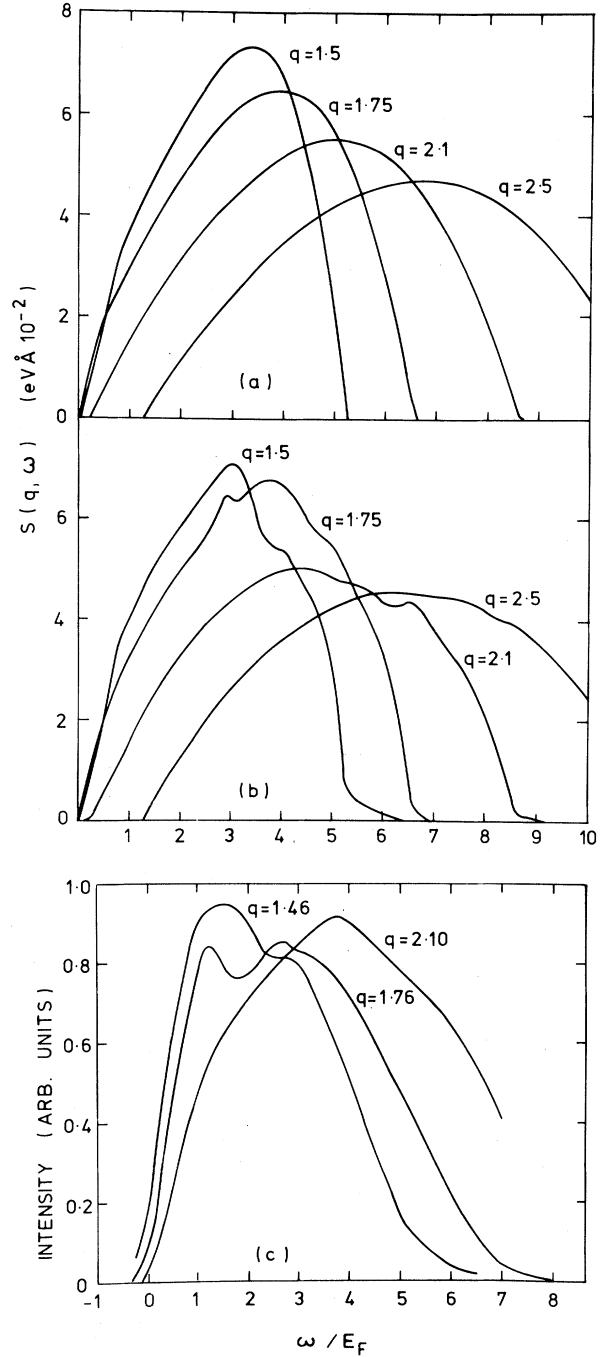


FIG. 2. Dynamic structure factor for fixed q/k_F . (a) RPA results; (b) present calculation; (c) intensity measurements for Be (Ref. 1).

relative effects over short distances of the Coulomb interaction.

The twin peaks shown are not significantly affected if in Eq. (3) we replace the denominator by the RPA denominator $[1 - v(\vec{q})\chi_0(\vec{q}, \omega)]$. We

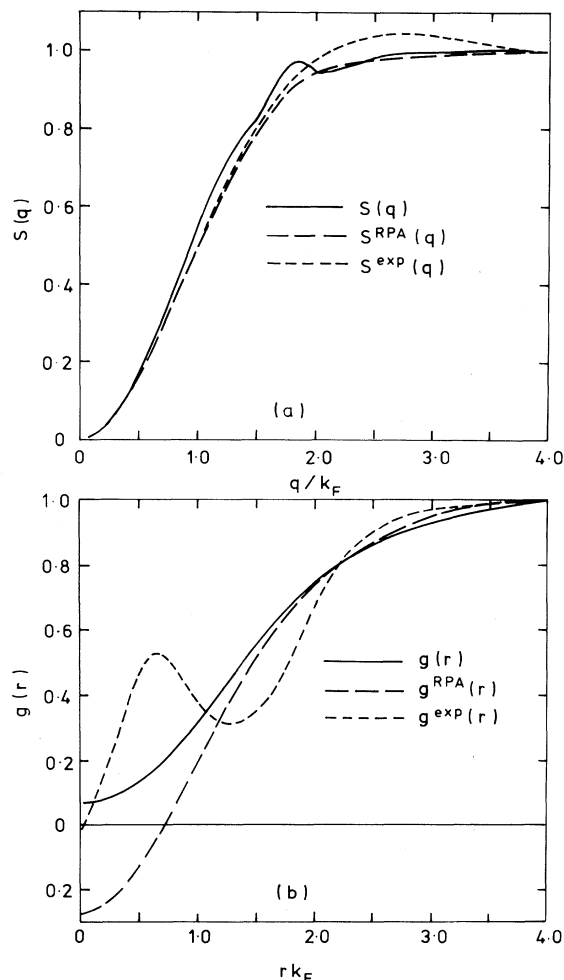


FIG. 3. (a) Static structure factor. (b) Pair correlation function.

conclude that the structure is generated purely by the behavior of $\chi_{sc}(\vec{q}, \omega)$ in the numerator of this expression, and in particular, that the twin peaks are not due to collective effects.

The experimental curves shown in Fig. 2 for comparison are those reported in Ref. 1 for beryllium. The ω scale used there indicates that the peaks measured for $q = 1.76$ and 2.10 lie to the left-hand side of the corresponding peaks in $\text{Im}\chi_0(\vec{q}, \omega)$ for the noninteracting system. The most probable explanation for this is that the ω scale contains a systematic error which is shifting it to the left. Thus in comparing the curves we have rigidly shifted the experimental figure to the right as shown.

The intensity scale for the experimental curves is in arbitrary units which are different for each q value, and so one should primarily compare

the position of the peaks. Our parameter-free microscopic calculation reproduces the main features of the measured ($q = 1.46$) and ($q = 1.76$) curves rather well. For the $q = 2.10$ curve, our central peak and also the RPA peak are both considerably broader than the measured peak. The secondary peak in our curve can be matched in the experimental curve to the slight shoulder on the right-hand side of the main peak. For $q = 2.5$ we obtain a single peak closely matching the RPA curve, which is as expected since for very large q , $\chi(\vec{q}, \omega) \cong \chi_0(\vec{q}, \omega)$.

Our total response function $\chi(\vec{q}, \omega)$ satisfies the f -sum rule and the conductivity sum rule⁸ numerically to better than 10%. The irreducible part of the response function $\chi_{sc}(\vec{q}, \omega)$ similarly satisfies the perfect screening and compressibility sum rules. We shall discuss elsewhere why our calculation may formally be expected to approximately preserve the conservation sum rules.

We perhaps should note that the twin-peak structure disappears if we use a dynamic local-field correction⁵ obtained by averaging⁷ our non-local t_{ee} .

The static structure factor $S(\vec{q})$ is given by

$$S(\vec{q}) = \rho^{-1} \int_0^\infty S(\vec{q}, \omega) d\omega, \quad (4)$$

where ρ is the electron density. Figure 3(a) shows our calculated $S(\vec{q})$, along with $S^{RPA}(\vec{q})$, obtained from the RPA, and a curve recently measured for beryllium,⁹ $S^{exp}(\vec{q})$. There is some evidence for a narrow maximum around $q \approx 1.8$ in our results, but the bump is very much less pronounced than the broad maximum in $S^{exp}(\vec{q})$.

The instantaneous pair correlation function $g(r)$ may be determined from $S(\vec{q})$ by using

$$g(r) - 1 = \frac{3}{2} r^{-1} \int_0^\infty q dq \sin qr [S(\vec{q}) - 1] \quad (5)$$

(with r in units of k_F^{-1}). Figure 3(b) shows our $g(r)$, $g^{RPA}(r)$ from the RPA, and $g^{exp}(r)$ from Eisenberger, Marra, and Brown.⁹ The form of our $g(r)$ is close to that obtained earlier⁷ and also to results based on a quite different set of corrections to χ_{sc} .¹⁰ This suggests, as it has been already pointed out,⁹ that the electron-gas model per se is probably unable to generate the peak seen in $g^{exp}(r)$, which occurs at a distance comparable to the radius of an ion core. We should also stress that the double-peak structure of $S(\vec{q}, \omega)$ has been obtained here without generating a peak in $g(r)$. Thus identifying the peak in $g^{exp}(r)$ with some core-electron effect⁹ becomes a very plausible assumption.

We wish to thank G. E. Brown and A. Sjölander for helpful discussions. This work was supported by an Australian Research Commission Grant.

¹P. M. Platzman and P. Eisenberger, Phys. Rev. Lett. **33**, 152 (1974).

²G. Mukhopadhyay, R. K. Kalia, and K. S. Singwi, Phys. Rev. Lett. **34**, 950 (1975); K. Awa, H. Yasuhara, and T. Asahi, Solid State Commun. **38**, 1285 (1981).

³H. De Raedt and B. De Raedt, Phys. Rev. B **18**, 2039 (1978).

⁴G. Mukhopadhyay and A. Sjölander, Phys. Rev. B **17**,

3589 (1978).

⁵K. Utsumi and S. Ichimaru, Phys. Rev. B **23**, 3291 (1981).

⁶B. K. Rao, S. S. Mandal, and D. N. Tripathy, Phys. Lett. **71A**, 447 (1979).

⁷D. N. Lowy and G. E. Brown, Phys. Rev. B **12**, 2438 (1975); K. Bedell and G. E. Brown, Phys. Rev. B **17**, 4512 (1978).

⁸See, e.g., D. Pines and P. Nozières, *Theory of Quantum Liquids* (Benjamin, New York, 1966).

⁹P. Eisenberger, W. C. Marra, and G. S. Brown, Phys. Rev. Lett. **45**, 1439 (1980).

¹⁰S. Mandal, B. K. Rao, and D. N. Tripathy, Phys. Rev. B **18**, 2524 (1978).

Ripplon-Limited Mobility of a Two-Dimensional Crystal of Electrons: Experiment

R. Mehrotra, B. M. Guenin,^(a) and A. J. Dahm

Department of Physics, Case Western Reserve University, Cleveland, Ohio 44106

(Received 24 August 1981)

A measurement of the mobility of a two-dimensional Wigner lattice supported by a liquid-helium surface is reported, and the results are compared with theory. The data exhibit a minimum in the mobility as a function of temperature. A narrow excess scattering peak located at or near the melting temperature is reminiscent of excess scattering associated with the dissociation of vortex-antivortex pairs in two-dimensional helium films and superconductors. Quantum corrections to the melting curve are observed.

PACS numbers: 73.20.-r, 63.20.-e, 64.70.Dv, 68.10.-m

A two-dimensional (2D) electron lattice supported by a liquid-helium surface forms an interesting and novel system. The simplicity of the interparticle interaction, the freedom from impurities, and a substrate which does not impose a regular potential on the lattice make this system an ideal prototype for the study of 2D lattices.

The scattering of phonons of the 2D electron lattice by liquid-helium ripplons can be investigated by measuring the mobility of an electron lattice supported by a liquid-helium substrate. Such data complement the information on the phonon-ripplon coupling provided by the experiment of Grimes and Adams¹ and the theory of Fisher, Halperin, and Platzman.² This measurement further probes the mean square electron displacement, $\langle x^2 \rangle$, which affects the coherence between ripplon crests and the electronic coordinates. Finally, an abrupt change in mobility upon crystallization allows for a precise measurement of the melting curve.

A cross section of our experimental cell, con-

sisting of a plane parallel capacitor with a plate separation of $s = 2$ mm, is shown in Fig. 1. Each plate has dimensions 18×25.4 mm² and is divided into three sections of equal area. A dc voltage is applied to the bottom plate to hold electrons against the helium surface, and the top plate is surrounded by guard electrodes used to shape the electron density profile. Electrons are deposited onto the surface from a glow discharge. All electrodes except B_1 and B_3 are at ac ground. An ac voltage of angular frequency ω applied to electrode B_1 causes a redistribution of the electrons, and a change in the density above electrode B_3 occurs after a time delay determined by the

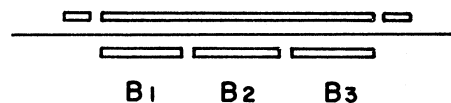


FIG. 1. A cross section of the experimental cell. The line between the plates represents the liquid level.